Appl Phys B (2010) 100: 597–609
DOI 10.1007/s00340-010-4125-4

Applied Physics B
Lasers and Optics

Scintillation calculations for partially coherent general beams via extended Huygens–Fresnel integral and self-designed Matlab function

H.T. Eyyuboğlu · Y. Baykal · Y. Cai

Received: 31 August 2009 / Revised version: 14 June 2010 / Published online: 2 July 2010

Abstract We present scintillation calculations in weak atmospheric turbulence for partially coherent general beams based on the extended Huygens–Fresnel integral and a Matlab function designed to handle expressions both of the average intensity and the average squared intensity. This way, the integrations are performed in a semi-analytic manner by the associated Matlab function, and this avoids lengthy, time-consuming and error prone hand derivations. The results are obtained for the partially coherent fundamental and higher-order sinusoidal and annular Gaussian beams. By plotting the scintillation index against the propagation distance and source size, we illustrate the on-axis scintillation behaviors of these beams. Accordingly, it is found that within specific source and parameter ranges, partially coherent fundamental, higher-order sinusoidal and annular Gaussian beams are capable of offering less scintillations, in comparison to the fundamental Gaussian beam.

1 Introduction

The existence of optical scintillation was suggested by Little [1]. The relevant mathematical formulation stipulates the solution of the wave equation for an inhomogeneous media. This is done via Rytov approximation, which expresses the receiver field in terms of expanded complex phase perturbations [2, 3]. Employing such a technique, Tatarski [4] and Fried [5] undertook the derivation of scintillation index for plane and spherical waves. The same was later extended to Gaussian beams by Ishimaru [6]. Goodman investigated the effects of scintillation on imaging [7]. Reference [8] is concerned with the inner scale measurements of turbulence, the modeling of the vertical turbulence strength (C_n^2) was carried out in [9]. Various scintillation measurements using spherical wave sources were performed over a horizontal path of 6 km and reported in [10]. For spherical waves, Hill and Clifford [11] put forward the theoretical formulation of strong turbulence, whilst comparing the theoretically derived results with those obtained from experimental observations. Transmitter aperture effects were analyzed in [12] for a Gaussian beam over vertical paths and for lidar applications in [13]. Taking horizontal and ground to satellite paths and plane wave propagation, bit error rate was formulated by Tyson [14] covering weak, moderate and strong turbulence regimes. Using two spherical wave sources at different wavelengths, scintillation correlation measurements were conducted [15]. The accuracy of acquiring wind velocity measurements from scintillation measurements were discussed in [16]. In [17], Tokovinin put forward the formulation of stellar scintillation index. Baker [18] developed a new scintillation calculation method to cope with the inadequacy of Rytov scintillation theory for some cases of focused Gaussian beams. It was shown in [19] how scintillations could be reduced via the utilization of multiwavelength Gaussian beam. For stratospheric turbulence, new power spectral models (other than Kolmogorov) were proposed in [20] and it was also shown that stratospheric turbulence mainly influenced phase fluctuations. In [21] Con-

H.T. Eyyuboğlu (✉) · Y. Baykal
Department of Electronic and Communication Engineering, Çankaya University, Öğretmenler Cad. No. 14 Yüzüncüyıl, 06530 Balgat, Ankara, Turkey
e-mail: h.eyyuboglu@cankaya.edu.tr
Fax: +90-312-2848043

Y. Baykal
e-mail: y.baykal@cankaya.edu.tr

Y. Cai
School of Physical Science and Technology, Soochow University, Suzhou 215006, China
e-mail: yangjian_cai@yahoo.com.cn

sortini and Conforti investigated the effect of detector saturation for small and large scales of scintillations. The effect of scintillations on the covariance of the received intensity of speckle pattern was discussed in [22]. Strong turbulence scintillation calculations were made in [23] and the results were compared to the previous works.

The scintillation index calculations in weak atmospheric turbulence are basically performed by employing the Rytov method as already stated above or by the extended Huygens–Fresnel integral. When different types of beams are considered, the Rytov method ends up with a solution that requires numerical or complex integration, which changes for each beam type [3, 24–37]. Here, a disadvantage arises due to the long computer run times involved as well as the fact that the numerical results obtained do not usually contain physical insights. Also, when source partial coherence is introduced in the scintillation calculations performed using the Rytov method, the solution cannot correctly predict the incoherent limit [38]. The alternative method used to obtain the scintillation index is the extended Huygens–Fresnel integral, which is employed by many researchers basically for the coherent [39–43] and partially coherent [44–48] Gaussian beams. Although the fundamental Gaussian beam is the most common output of lasers, for some practical applications it is desirable to have multiple beam configurations [3, 49, 50]. In most cases, beams other than the fundamental Gaussian beam are found to have less scintillations within certain source and propagation parameter ranges [24, 27–37, 49]. Recently, using the extended Huygens–Fresnel integral, we have formulated and evaluated the scintillation indices in weak atmospheric turbulence of different types of partially coherent beams such as multiple Gaussian [51], off-axis [52], cos and cosh Gaussian [53]. In the current paper, we study the scintillation properties in weak atmospheric turbulence of partially coherent general beams using the extended Huygens–Fresnel integral and a self-designed Matlab function. Through these evaluations we are able to acquire the scintillation indices of partially coherent higher-order beams and their fundamental versions of sinusoidal Gaussian and annular types. The advantage of the procedure followed in the present paper is that when structure and correlation functions are approximated by quadratic powers, the scintillation index of a large class of beams can be treated in an analytical form and through the use of the self-designed Matlab function, scintillation indices of many beams can be obtained by appropriately organizing in matrix form the relevant coefficients appearing in the integrands of the average intensity and average squared intensity expressions.

Summarizing we can say that, into the context of the existing literature, the current work introduces two new and distinct features. The first one is the application of self-designed Matlab function to the scintillation index calculations involving extended Huygens–Fresnel integrals. The second is the investigation of scintillation characteristics of higher-order sinusoidal and annular Gaussian beams. We stress that theses two topics are totally new from the existing literature point of view.

2 Preparation of matrices for the Matlab function

A higher-order general beam involving Gaussian exponentials, complex displacement parameters and Hermite polynomials can be stated in the form of the following summation [54]

$$u_s(s_x, s_y) = \sum_{\ell=1}^{N} A_\ell \exp\left[-0.5k\left(\alpha_{x\ell} s_x^2 + \alpha_{y\ell} s_y^2\right)\right] \times \exp\left[-j\left(V_{x\ell} s_x + V_{y\ell} s_y\right)\right] \times H_{mx\ell}(a_{x\ell} s_x) H_{my\ell}(a_{y\ell} s_y) \tag{1}$$

where the transverse source plane coordinates are s_x and s_y, the number of beams to be used in the composition of the general beam is N, and the amplitude factor, which can be different for each ℓth component of the source field, is shown by A_ℓ. $k = 2\pi/\lambda$ indicates the wave number, with λ being the wavelength. The beam profile of (1) is collectively determined by the Gaussian exponential, $\exp[-0.5k(\alpha_{x\ell} s_x^2 + \alpha_{y\ell} s_y^2)]$, with $\alpha_{x\ell}$ and $\alpha_{y\ell}$ being related to source sizes $\alpha_{sx\ell}$, $\alpha_{sy\ell}$ and the focusing parameters $F_{x\ell}$, $F_{y\ell}$ in the manner $\alpha_{x\ell} = 1/(k\alpha_{sx\ell}^2) + j/F_{x\ell}$, $\alpha_{y\ell} = 1/(k\alpha_{sy\ell}^2) + j/F_{y\ell}$, by the displacement exponential $\exp[-j(V_{x\ell} s_x + V_{y\ell} s_y)]$, where $V_{x\ell}$, $V_{y\ell}$ serve to create phase rotation as well as physical displacements and finally by the Hermite polynomials, $H_{mx\ell}(a_{x\ell} s_x)$ and $H_{my\ell}(a_{y\ell} s_y)$, with $mx\ell$ and $my\ell$ being the orders, $a_{x\ell}$ and $a_{y\ell}$ indicating the widths [55, 56]. The style of the expression in (1) allows us to set x and y components independently. It is possible to achieve cos, cosh, sine, sinh, annular Gaussian beams and their higher-order counterparts from (1) via the arrangements of source parameters as explained in [55].

The representation in (1) can be converted into a partially coherent beam using the Gaussian Schell model [3] and assigning a partial coherence parameter denoted by σ_s. Expressing the result in terms of the mutual coherence function, we get [57]

$$\begin{aligned}\Gamma_s(s_{1x}, s_{2x}, s_{1y}, s_{2y}) &= u_s(s_{1x}, s_{1y}) u_s^*(s_{2x}, s_{2y}) \\ &\quad \times \exp\left[-\frac{0.5}{\sigma_s^2}\left(s_{1x}^2 + s_{2x}^2 - 2s_{1x}s_{2x} + s_{1y}^2 + s_{2y}^2 - 2s_{1y}s_{2y}\right)\right]\end{aligned} \tag{2}$$

where $*$ means the complex conjugate.

To find the average intensity, (2) has to be inserted into the extended Huygens–Fresnel integral. When one replaces $u_s()$ in (2) with the definition given in (1), for a receiver plane having the transverse coordinates of r_x, r_y, the extended Huygens–Fresnel integral will appear as

$$\begin{aligned}
&\langle I(r_x, r_y, L)\rangle \\
&= \frac{k^2}{(2\pi L)^2} \sum_{\ell_1=1}^{N} \sum_{\ell_2=1}^{N} A_{\ell_1} A_{\ell_2}^* \\
&\quad \times \int_{-\infty}^{\infty} \int_{-\infty}^{\infty} \int_{-\infty}^{\infty} \int_{-\infty}^{\infty} ds_{1x}\, ds_{2x}\, ds_{1y}\, ds_{2y} \\
&\quad \times \exp\big[-0.5k\big(\alpha_{x\ell_1} s_{1x}^2 + \alpha_{x\ell_2}^* s_{2x}^2 \\
&\quad + \alpha_{y\ell_1} s_{1y}^2 + \alpha_{y\ell_2}^* s_{2y}^2\big)\big] \\
&\quad \times \exp\big[-\big(jV_{x\ell_1} s_{1x} - jV_{x\ell_2}^* s_{2x} \\
&\quad + jV_{y\ell_1} s_{1y} - jV_{y\ell_2}^* s_{2y}\big)\big] \\
&\quad \times H_{mx\ell_1}(a_{x\ell_1} s_{1x}) H_{mx\ell_2}(a_{x\ell_2} s_{2x}) H_{my\ell_1}(a_{y\ell_1} s_{1y}) \\
&\quad \times H_{my\ell_2}(a_{y\ell_2} s_{2y}) \\
&\quad \times \exp\bigg[-\frac{0.5}{\sigma_s^2}\big(s_{1x}^2 + s_{2x}^2 - 2s_{1x}s_{2x} + s_{1y}^2 \\
&\quad + s_{2y}^2 - 2s_{1y}s_{2y}\big)\bigg] \\
&\quad \times \exp\bigg[\frac{0.5jk}{L}\big(s_{1x}^2 - s_{2x}^2 - 2r_x s_{1x} + 2r_x s_{2x} \\
&\quad + s_{1y}^2 - s_{2y}^2 - 2r_y s_{1y} + 2r_y s_{2y}\big)\bigg] \\
&\quad \times \exp\bigg[-\frac{1}{\rho_0^2}\big(s_{1x}^2 + s_{2x}^2 - 2s_{1x}s_{2x} + s_{1y}^2 \\
&\quad + s_{2y}^2 - 2s_{1y}s_{2y}\big)\bigg] \qquad (3)
\end{aligned}$$

Here the distance from the source to receiver plane is L, the coherence length of a spherical wave propagating in turbulence is $\rho_0 = (0.545 C_n^2 k^2 L)^{-3/5}$, with C_n^2 referring to the structure constant. Here we note that, since C_n^2 is taken to be uniform along the propagation path, our results will be limited to short horizontal paths. In (3), the diffraction and turbulence effects are taken into account via the last two exponentials.

To solve an integral of the type given in (3) with the help of our Matlab function, firstly a matching process has to be applied between (3) and the expression below:

$$\begin{aligned}
I &= \int_{-\infty}^{\infty} \int_{-\infty}^{\infty} \int_{-\infty}^{\infty} \int_{-\infty}^{\infty} dt_1\, dt_2\, dt_3\, dt_4 \\
&\quad \times \exp\big(-q_{11}t_1^2 - q_{22}t_2^2 - q_{33}t_3^2 - q_{44}t_4^2\big) \\
&\quad \times H_{m_1}(c_1t_1) H_{m_2}(c_2t_2) H_{m_3}(c_3t_3) H_{m_4}(c_4t_4) \\
&\quad \times \exp(-2q_{12}t_1t_2 - 2q_{13}t_1t_3 - 2q_{14}t_1t_4 \\
&\quad - 2q_{23}t_2t_3 - 2q_{24}t_2t_4 - 2q_{34}t_3t_4) \\
&\quad \times \exp(-2r_1t_1 - 2r_2t_2 - 2r_3t_3 - 2r_4t_4) t_1^{n_1} t_2^{n_2} t_3^{n_3} t_4^{n_4} \qquad (4)
\end{aligned}$$

When one associates the variables of (4), i.e., t_1, t_2, t_3, t_4 with the variables of (3), i.e. s_{1x}, s_{2x}, s_{1y}, s_{2y}, respectively, equating the corresponding coefficients and arranging all the terms in matrix form will generate the following identities:

$$\mathbf{Q} = \begin{pmatrix} q_{11} & q_{12} & q_{13} & q_{14} \\ q_{12} & q_{22} & q_{23} & q_{24} \\ q_{13} & q_{23} & q_{33} & q_{34} \\ q_{14} & q_{24} & q_{34} & q_{44} \end{pmatrix}$$

$$= \begin{pmatrix} 0.5k\alpha_{x\ell_1} + \frac{0.5}{\sigma_s^2} - \frac{0.5jk}{L} + \frac{1}{\rho_0^2} & -\frac{0.5}{\sigma_s^2} - \frac{1}{\rho_0^2} & 0 & 0 \\ -\frac{0.5}{\sigma_s^2} - \frac{1}{\rho_0^2} & 0.5k\alpha_{x\ell_2}^* + \frac{0.5}{\sigma_s^2} + \frac{0.5jk}{L} + \frac{1}{\rho_0^2} & 0 & 0 \\ 0 & 0 & 0.5k\alpha_{y\ell_1} + \frac{0.5}{\sigma_s^2} - \frac{0.5jk}{L} + \frac{1}{\rho_0^2} & -\frac{0.5}{\sigma_s^2} - \frac{1}{\rho_0^2} \\ 0 & 0 & -\frac{0.5}{\sigma_s^2} - \frac{1}{\rho_0^2} & 0.5k\alpha_{y\ell_2}^* + \frac{0.5}{\sigma_s^2} + \frac{0.5jk}{L} + \frac{1}{\rho_0^2} \end{pmatrix} \qquad (5a)$$

$$\mathbf{R} = \begin{pmatrix} r_1 & r_2 & r_3 & r_4 \end{pmatrix}$$

$$= \begin{pmatrix} 0.5jV_{x\ell_1} + \frac{0.5jkr_x}{L} & -0.5jV_{x\ell_2}^* - \frac{0.5jkr_x}{L} & 0.5jV_{y\ell_1} + \frac{0.5jkr_y}{L} & -0.5jV_{y\ell_2}^* - \frac{0.5jkr_y}{L} \end{pmatrix} \qquad (5b)$$

$$\mathbf{N} = \begin{pmatrix} n_1 & n_2 & n_3 & n_4 \end{pmatrix} = \begin{pmatrix} 0 & 0 & 0 & 0 \end{pmatrix} \qquad (5c)$$

$$\mathbf{M} = \begin{pmatrix} m_1 & m_2 & m_3 & m_4 \\ c_1 & c_2 & c_3 & c_4 \end{pmatrix} = \begin{pmatrix} mx\ell_1 & mx\ell_2 & my\ell_1 & my\ell_2 \\ a_{x\ell_1} & a_{x\ell_2} & a_{y\ell_1} & a_{y\ell_2} \end{pmatrix} \tag{5d}$$

Preparing the matrices **Q**, **R**, **N**, **M** in the ways described in (5) and then placing them into arguments of the Matlab function as described at length in [58] we accomplish the evaluation of (3), yielding the average intensity $\langle I(r_x, r_y, L)\rangle$. It is worth noting that the evaluation performed by our Matlab function does in no way imply a numeric integration of (3), but it rather represents an exact result, completely analogous to an analytic solution of the quadruple integral in (3) [58].

The average squared on-axis intensity can be written by benefiting from the on-axis fourth order coherence function [51].

$$\begin{aligned}
\langle I^2(0,0,L)\rangle &= \frac{k^4}{(2\pi L)^4} \sum_{\ell_1=1}^{N} \sum_{\ell_2=1}^{N} \sum_{\ell_3=1}^{N} \sum_{\ell_4=1}^{N} A_{\ell_1} A_{\ell_2}^* A_{\ell_3} A_{\ell_4}^* \int_{-\infty}^{\infty}\int_{-\infty}^{\infty}\int_{-\infty}^{\infty}\int_{-\infty}^{\infty} ds_{1x}\, ds_{2x}\, ds_{3x}\, ds_{4x} \\
&\times \exp\left[-0.5k\left(\alpha_{x\ell_1} s_{1x}^2 + \alpha_{x\ell_2}^* s_{2x}^2 + \alpha_{x\ell_3} s_{3x}^2 + \alpha_{x\ell_4}^* s_{4x}^2\right)\right] \\
&\times \exp\left[-\left(jV_{x\ell_1} s_{1x} - jV_{x\ell_2}^* s_{2x} + jV_{x\ell_3} s_{3x} - jV_{x\ell_4}^* s_{4x}\right)\right] \\
&\times H_{mx\ell_1}(a_{x\ell_1} s_{1x}) H_{mx\ell_2}(a_{x\ell_2} s_{2x}) H_{mx\ell_3}(a_{x\ell_3} s_{3x}) H_{x\ell_4}(a_{x\ell_4} s_{4x}) \\
&\times \exp\left[-\frac{0.5}{\sigma_s^2}\left(s_{1x}^2 + s_{2x}^2 + s_{3x}^2 + s_{4x}^2 - 2s_{1x}s_{2x} - 2s_{3x}s_{4x}\right)\right] \exp\left[\frac{0.5jk}{L}\left(s_{1x}^2 - s_{2x}^2 + s_{3x}^2 - s_{4x}^2\right)\right] \\
&\times \exp\left[-\frac{j}{\rho_{\chi s}^2}\left(s_{1x}^2 - s_{2x}^2 + s_{3x}^2 - s_{4x}^2 - 2s_{1x}s_{3x} + 2s_{2x}s_{4x}\right)\right] \\
&\times \left\{\exp\left[-\frac{1}{\rho_0^2}\left(s_{1x}^2 + s_{2x}^2 + s_{3x}^2 + s_{4x}^2 - 2s_{1x}s_{2x} + 2s_{1x}s_{3x} - 2s_{1x}s_{4x} - 2s_{2x}s_{3x} + 2s_{2x}s_{4x} - 2s_{3x}s_{4x}\right)\right]\right. \\
&+ 2\sigma_\chi^2 \exp\left[-\frac{1}{\rho_0^2}\left(2s_{1x}^2 + s_{2x}^2 + 2s_{3x}^2 + s_{4x}^2 - 2s_{1x}s_{2x} - 2s_{1x}s_{4x} - 2s_{2x}s_{3x} + 2s_{2x}s_{4x} - 2s_{3x}s_{4x}\right)\right] \\
&\left.+ 2\sigma_\chi^2 \exp\left[-\frac{1}{\rho_0^2}\left(s_{1x}^2 + 2s_{2x}^2 + s_{3x}^2 + 2s_{4x}^2 - 2s_{1x}s_{2x} + 2s_{1x}s_{3x} - 2s_{1x}s_{4x} - 2s_{2x}s_{3x} - 2s_{3x}s_{4x}\right)\right]\right\} \\
&\bullet \int_{-\infty}^{\infty}\int_{-\infty}^{\infty}\int_{-\infty}^{\infty}\int_{-\infty}^{\infty} ds_{1y}\, ds_{2y}\, ds_{3y}\, ds_{4y} \exp\left[-0.5k\left(\alpha_{y\ell_1} s_{1y}^2 + \alpha_{y\ell_2}^* s_{2y}^2 + \alpha_{y\ell_3} s_{3y}^2 + \alpha_{y\ell_4}^* s_{4y}^2\right)\right] \\
&\times \exp\left[-\left(jV_{y\ell_1} s_{1y} - jV_{y\ell_2}^* s_{2y} + jV_{y\ell_3} s_{3y} - jV_{y\ell_4}^* s_{4y}\right)\right] \\
&\times H_{my\ell_1}(a_{y\ell_1} s_{1y}) H_{my\ell_2}(a_{y\ell_2} s_{2y}) H_{my\ell_3}(a_{y\ell_3} s_{3y}) H_{y\ell_4}(a_{y\ell_4} s_{4y}) \\
&\times \exp\left[-\frac{0.5}{\sigma_s^2}\left(s_{1y}^2 + s_{2y}^2 + s_{3y}^2 + s_{4y}^2 - 2s_{1y}s_{2y} - 2s_{3y}s_{4y}\right)\right] \exp\left[\frac{0.5jk}{L}\left(s_{1y}^2 - s_{2y}^2 + s_{3y}^2 - s_{4y}^2\right)\right] \\
&\times \exp\left[-\frac{j}{\rho_{\chi s}^2}\left(s_{1y}^2 - s_{2y}^2 + s_{3y}^2 - s_{4y}^2 - 2s_{1y}s_{3y} + 2s_{2y}s_{4y}\right)\right] \\
&\times \left\{\exp\left[-\frac{1}{\rho_0^2}\left(s_{1y}^2 + s_{2y}^2 + s_{3y}^2 + s_{4y}^2 - 2s_{1y}s_{2y} + 2s_{1y}s_{3y} - 2s_{1y}s_{4y} - 2s_{2y}s_{3y} + 2s_{2y}s_{4y} - 2s_{3y}s_{4y}\right)\right]\right. \\
&+ 2\sigma_\chi^2 \exp\left[-\frac{1}{\rho_0^2}\left(2s_{1y}^2 + s_{2y}^2 + 2s_{3y}^2 + s_{4y}^2 - 2s_{1y}s_{2y} - 2s_{1y}s_{4y} - 2s_{2y}s_{3y} + 2s_{2y}s_{4y} - 2s_{3y}s_{4y}\right)\right] \\
&\left.+ 2\sigma_\chi^2 \exp\left[-\frac{1}{\rho_0^2}\left(s_{1y}^2 + 2s_{2y}^2 + s_{3y}^2 + 2s_{4y}^2 - 2s_{1y}s_{2y} + 2s_{1y}s_{3y} - 2s_{1y}s_{4y} - 2s_{2y}s_{3y} - 2s_{3y}s_{4y}\right)\right]\right\}
\end{aligned} \tag{6}$$

where the variance of log amplitude for spherical waves is $\sigma_\chi^2 = 0.124 C_n^2 k^{7/6} L^{11/6}$ and the coherence length of log amplitude and phase is $\rho_{\chi S} = (0.1134 k^{13/6} C_n^2 L^{5/6})^{-1/2}$. We have been able to split (6) into a product of two independent quadruple integrals because of the absence of coupling between the x and y components. Using this property, it is possible to treat the matching process of (6) to (3) as two independent operations, i.e. one operation for x components, the other for y components. Furthermore, each integrand part of (6) comprises three summations such that

$$\begin{aligned}\left\langle I^2(0,0,L)\right\rangle &= (I_{Ax} + I_{Bx} + I_{Cx}) \bullet (I_{Ay} + I_{By} + I_{Cy}) \\ &= I_{Ax} I_{Ay} + I_{Bx} I_{By} + I_{Cx} I_{Cy}\end{aligned} \quad (7)$$

where the A, B and C indexing results from the existence of three exponentials within the curly brackets at the end of the integration with respect to the x or y variables. With these details in mind, the matching actions between (6) and (3) are now implemented, eventually delivering the **Q**, **R**, **N**, **M** matrices that will be used in the arguments of the Matlab function for the evaluation of (6). These matrices are displayed in (8) along with some information on how to generate the other cases, which are not directly exhibited in (8) for reasons of saving space. In addition to the information provided, we note that for the matrices of (8) there is no variation in **R** and **M** with A, B and C indexing while, on the other hand, the y counterparts of all matrices are simply obtained by changing the x indexed terms to y indexed ones as illustrated for the **R** and **M** matrices.

$$\mathbf{Q}_x = \begin{pmatrix} 0.5k\alpha_{x\ell_1} + \frac{0.5}{\sigma_s^2} - \frac{0.5jk}{L} + \frac{j}{\rho_{\chi s}^2} + \frac{q_{11\rho_0^2}}{\rho_0^2} & -\frac{0.5}{\sigma_s^2} - \frac{1}{\rho_0^2} & -\frac{j}{\rho_{\chi s}^2} + \frac{q_{13\rho_0^2}}{\rho_0^2} & -\frac{1}{\rho_0^2} \\ -\frac{0.5}{\sigma_s^2} - \frac{1}{\rho_0^2} & 0.5k\alpha_{x\ell_2}^* + \frac{0.5}{\sigma_s^2} + \frac{0.5jk}{L} - \frac{j}{\rho_{\chi s}^2} + \frac{q_{22\rho_0^2}}{\rho_0^2} & -\frac{1}{\rho_0^2} & \frac{j}{\rho_{\chi s}^2} + \frac{q_{24\rho_0^2}}{\rho_0^2} \\ -\frac{j}{\rho_{\chi s}^2} + \frac{q_{13\rho_0^2}}{\rho_0^2} & -\frac{1}{\rho_0^2} & 0.5k\alpha_{x\ell_3} + \frac{0.5}{\sigma_s^2} - \frac{0.5jk}{L} + \frac{j}{\rho_{\chi s}^2} + \frac{q_{11\rho_0^2}}{\rho_0^2} & -\frac{0.5}{\sigma_s^2} - \frac{1}{\rho_0^2} \\ -\frac{1}{\rho_0^2} & \frac{j}{\rho_{\chi s}^2} + \frac{q_{24\rho_0^2}}{\rho_0^2} & -\frac{0.5}{\sigma_s^2} - \frac{1}{\rho_0^2} & 0.5k\alpha_{x\ell_4}^* + \frac{0.5}{\sigma_s^2} + \frac{0.5jk}{L} - \frac{j}{\rho_{\chi s}^2} + \frac{q_{22\rho_0^2}}{\rho_0^2} \end{pmatrix}$$

$$q_{11\rho_0^2} = \begin{cases} 1 & \text{for } \mathbf{Q}_{Ax} \text{ and } \mathbf{Q}_{Cx} \\ 2 & \text{for } \mathbf{Q}_{Bx} \end{cases}, \qquad q_{13\rho_0^2} = \begin{cases} 1 & \text{for } \mathbf{Q}_{Ax} \text{ and } \mathbf{Q}_{Cx} \\ 0 & \text{for } \mathbf{Q}_{Bx} \end{cases},$$

$$q_{22\rho_0^2} = \begin{cases} 1 & \text{for } \mathbf{Q}_{Ax} \text{ and } \mathbf{Q}_{Bx} \\ 2 & \text{for } \mathbf{Q}_{Cx} \end{cases}, \qquad q_{24\rho_0^2} = \begin{cases} 1 & \text{for } \mathbf{Q}_{Ax} \text{ and } \mathbf{Q}_{Bx} \\ 0 & \text{for } \mathbf{Q}_{Cx} \end{cases} \quad (8a)$$

$$\begin{aligned}\mathbf{R}_x &= \begin{pmatrix} 0.5jV_{x\ell_1} & -0.5jV_{x\ell_2}^* & 0.5jV_{x\ell_3} & -0.5jV_{x\ell_4}^* \end{pmatrix} \\ \mathbf{R}_y &= \begin{pmatrix} 0.5jV_{y\ell_1} & -0.5jV_{y\ell_2}^* & 0.5jV_{y\ell_3} & -0.5jV_{y\ell_4}^* \end{pmatrix}\end{aligned} \quad (8b)$$

$$\mathbf{N} = \begin{pmatrix} 0 & 0 & 0 & 0 \end{pmatrix} \quad (8c)$$

$$\begin{aligned}\mathbf{M}_x &= \begin{pmatrix} mx\ell_1 & mx\ell_2 & mx\ell_3 & my\ell_4 \\ a_{x\ell_1} & a_{x\ell_2} & a_{x\ell_3} & a_{x\ell_4} \end{pmatrix} \\ \mathbf{M}_y &= \begin{pmatrix} my\ell_1 & my\ell_2 & my\ell_3 & my\ell_4 \\ a_{y\ell_1} & a_{y\ell_2} & a_{y\ell_3} & a_{y\ell_4} \end{pmatrix}\end{aligned} \quad (8d)$$

Upon evaluating the averaged intensity given in (3) and the average squared intensity given in (6) by submitting the above derived matrices to our Matlab function, as described in [58], we are able to arrive at the on-axis scintillation index of the general beam of (1) using the following relation

$$m^2 = \frac{\langle I^2(0,0,L)\rangle}{\langle I(0,0L)\rangle^2} - 1 \quad (9)$$

3 Graphical outputs

In this section we analyze the scintillation characteristics in weak atmospheric turbulence of collimated partially coherent higher-order cos, cosh, annular, sin and sinh Gaussian beams at various propagation distances, displacement parameters, amplitude ratios, partial coherence degrees and source sizes. To this end, we fix the remaining

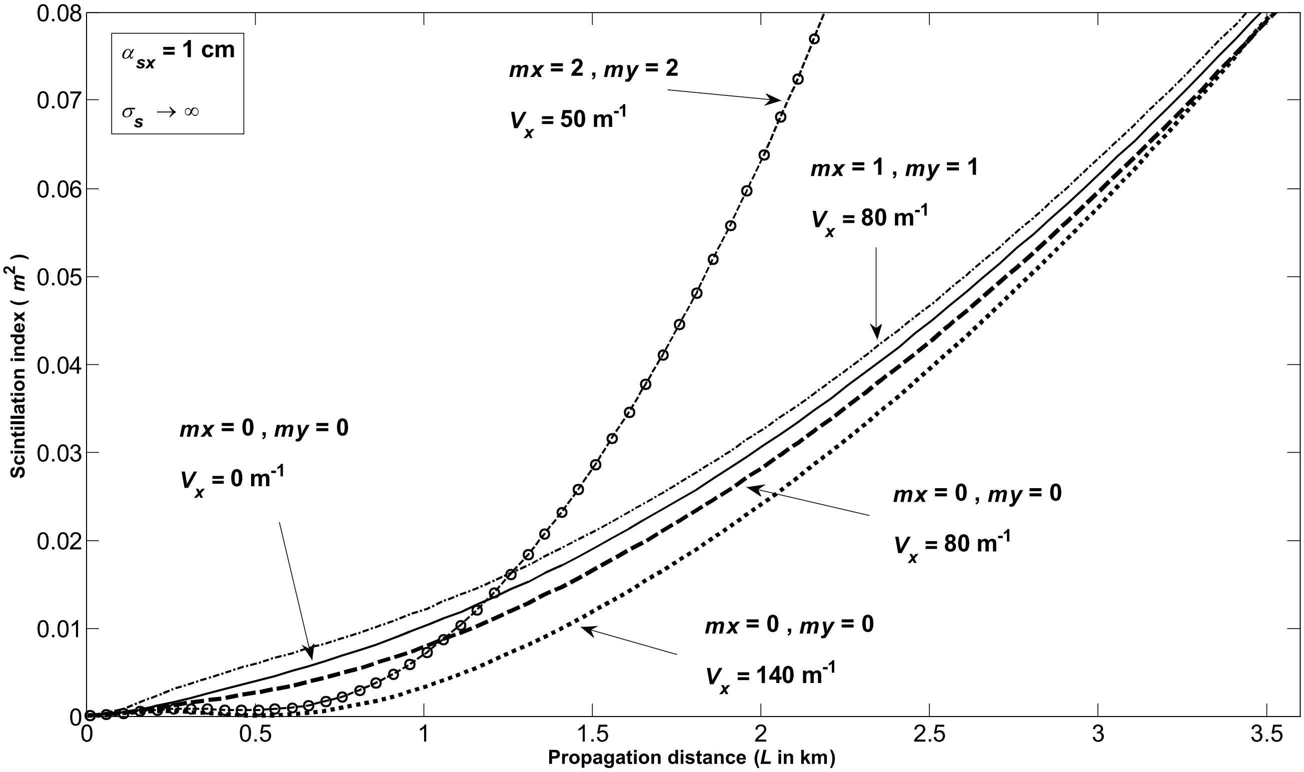

Fig. 1 Scintillation index behavior of fully coherent higher-order cos Gaussian beams against propagation distance

parameters as $a_{x\ell} = a_{y\ell} = 1/\alpha_{sx} = 1/\alpha_{sy}$, $\lambda = 1.55$ μm, $C_n^2 = 10^{-15}$ m$^{-2/3}$ and assume x–y symmetric source sizes and displacement parameters. Note that the different beam arrangements are shown in Table 1 of [55]. The graphical outputs are produced with the use of (9) that requires the submission of **Q**, **R**, **M** matrices to the Matlab function using the procedures described in Sect. 2.

By letting σ_s be infinity, i.e., taking fully coherent beams, Fig. 1 shows that at the selected source size of $\alpha_{sx} = 1$ cm, the cos Gaussian beams, compared to the Gaussian beam indicated by $mx = 0$, $my = 0$, $V_x = 0$, will have less on-axis scintillations as the magnitude of the displacement is increased, except for the higher-order cases, where a lower trend is initially observed at shorter propagation distances for $mx = 2$, $my = 2$, $V_x = 50$ m^{-1}. Next we examine the higher-order cosh Gaussian beams in Fig. 2, under the same circumstances as those of Fig. 1. It is seen from Fig. 2 that cosh Gaussian beams act in a reverse manner to cos Gaussian beams as also noted in earlier investigations [28, 30], i.e., the scintillations of cosh Gaussian beam will rise as the displacement parameter becomes bigger, while the higher-order versions tend to possess higher scintillations than the fundamental ones. Figure 3 illustrates the case of higher-order annular Gaussian beams at several amplitude factors and order numbers. Figure 3 demonstrates that, compared to the Gaussian beam marked by $mx = 0$, $my = 0$, $A_1 = 1$, $A_2 = 0$, the higher-order annular Gaussian beams will scintillate less than the fundamental annular Gaussian ones, whereas the smaller amplitude factor of the secondary beam (A_2) will lead to a slight escalation in scintillations.

Now we turn to partially higher-order coherent beams. In Fig. 4, the beams of Fig. 3 are plotted at $\sigma_s = 10^{-3}$ cm. Figure 3 shows that at such a low coherence setting, the scintillations curves for all annular Gaussian beams come close to each other, with the respective positions of higher-order beams being retained but with the fundamental ones falling below the Gaussian beam.

For sine and sinh Gaussian beams, we also opt for the partially coherent types. With a source size of $\alpha_{sx} = 5$ cm, Fig. 5 displays the variation of several sine Gaussian beams against propagation distance. Just like the cos Gaussian beam, it is seen from Fig. 5 that raising the displacement parameter helps to reduce scintillations of sine Gaussian beams. On the other hand, according to Fig. 5, increased orders seem to generate more scintillation if the partial coherence parameter σ_s is kept constant at 1 cm, but lowering σ_s to 10^{-3} cm certainly results in a substantial decrease of scintillations of the sine Gaussian beam. In Fig. 6 we observe a behavior of sinh Gaussian beams similar to the cosh beam case of Fig. 2. Thus, there is a rising trend of scintillations with increasing displacement parameter values, while higher orders also seem to cause more scintillations.

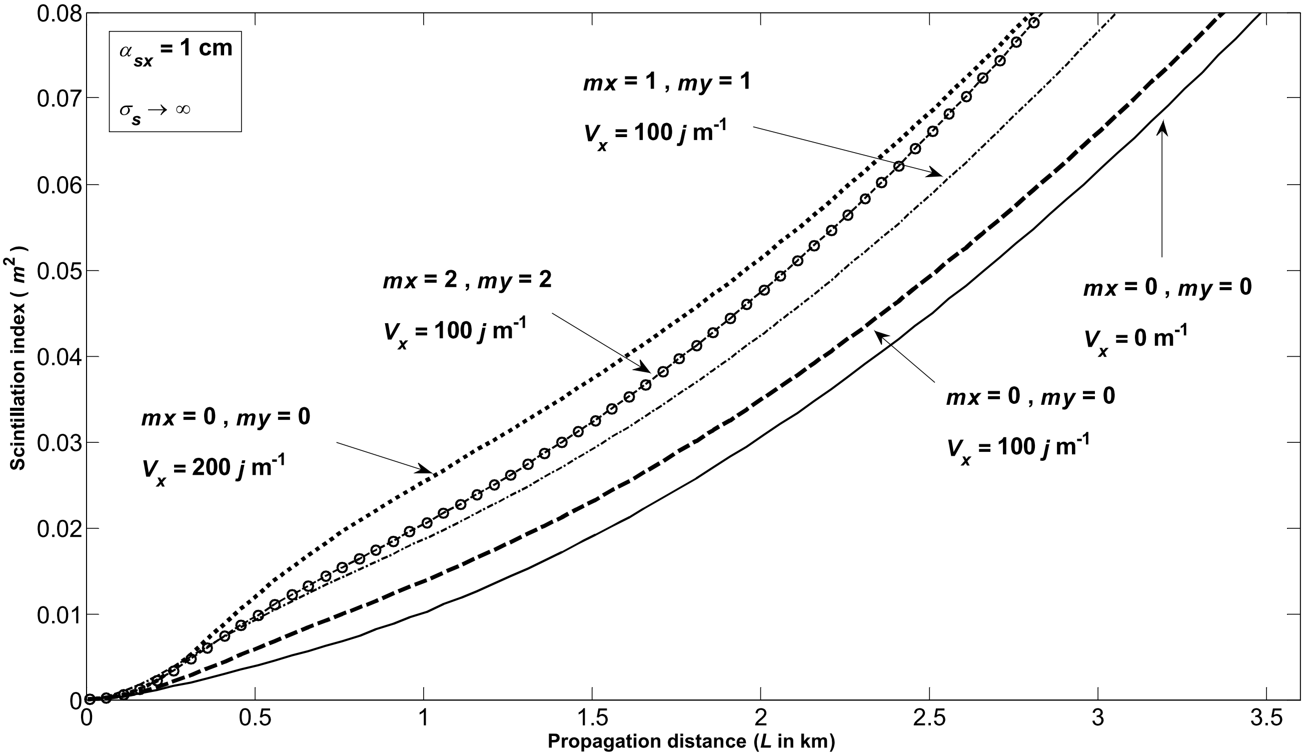

Fig. 2 Scintillation index behavior of fully coherent higher-order cosh Gaussian beams against propagation distance

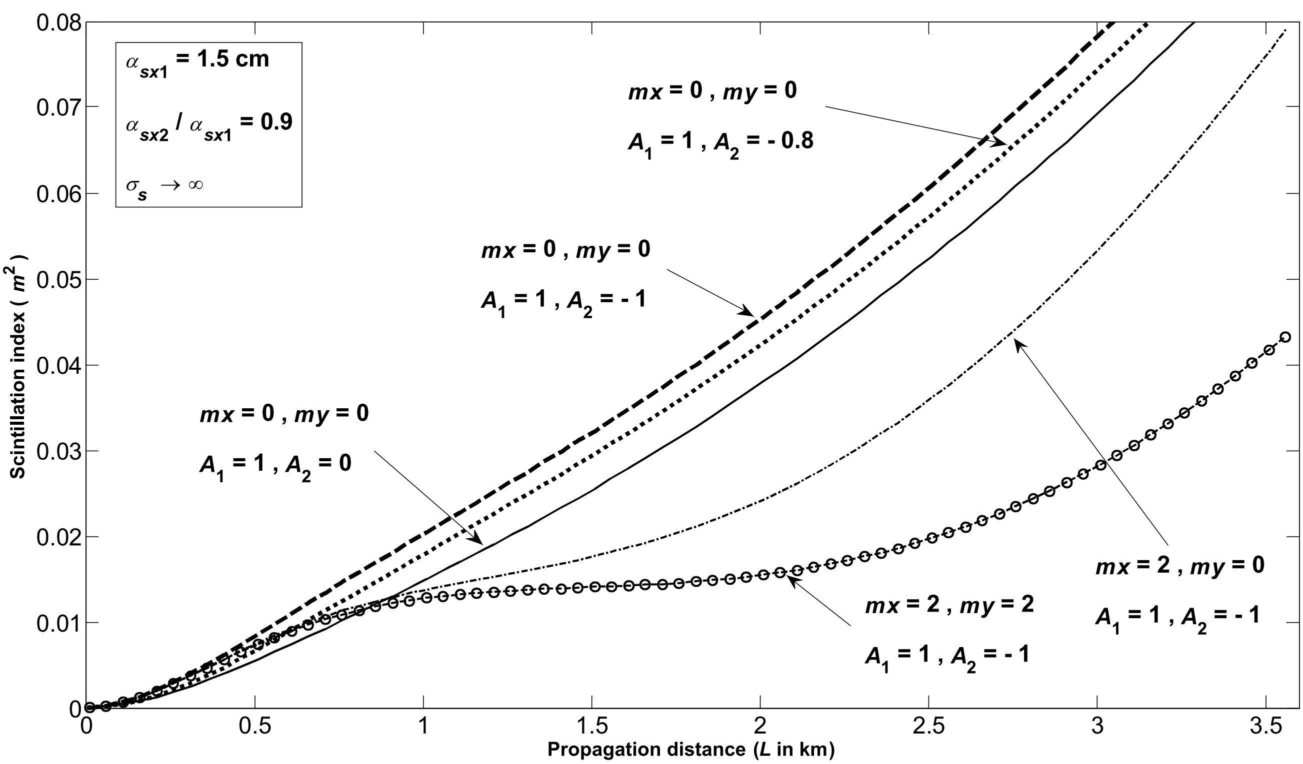

Fig. 3 Scintillation index behavior of fully coherent higher-order annular Gaussian beams against propagation distance

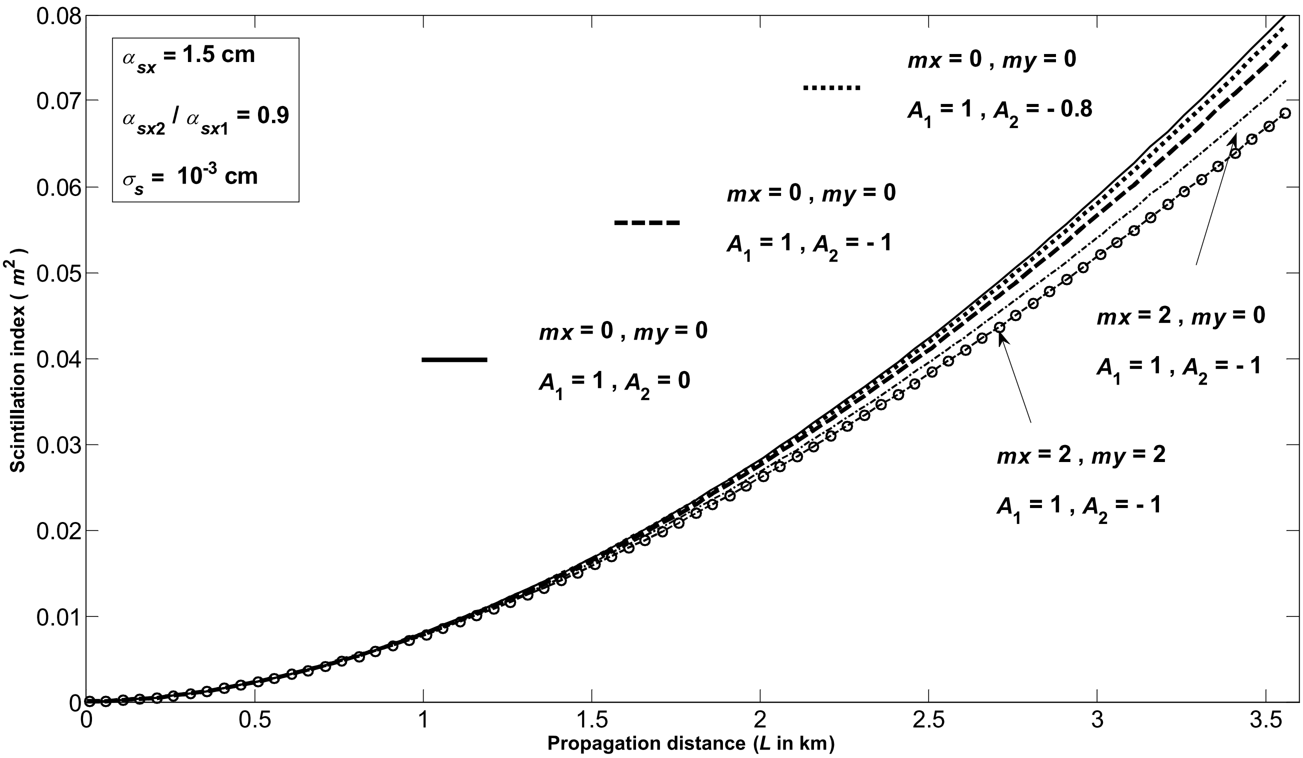

Fig. 4 Scintillation index behavior of partially coherent higher-order annular Gaussian beams against propagation distance

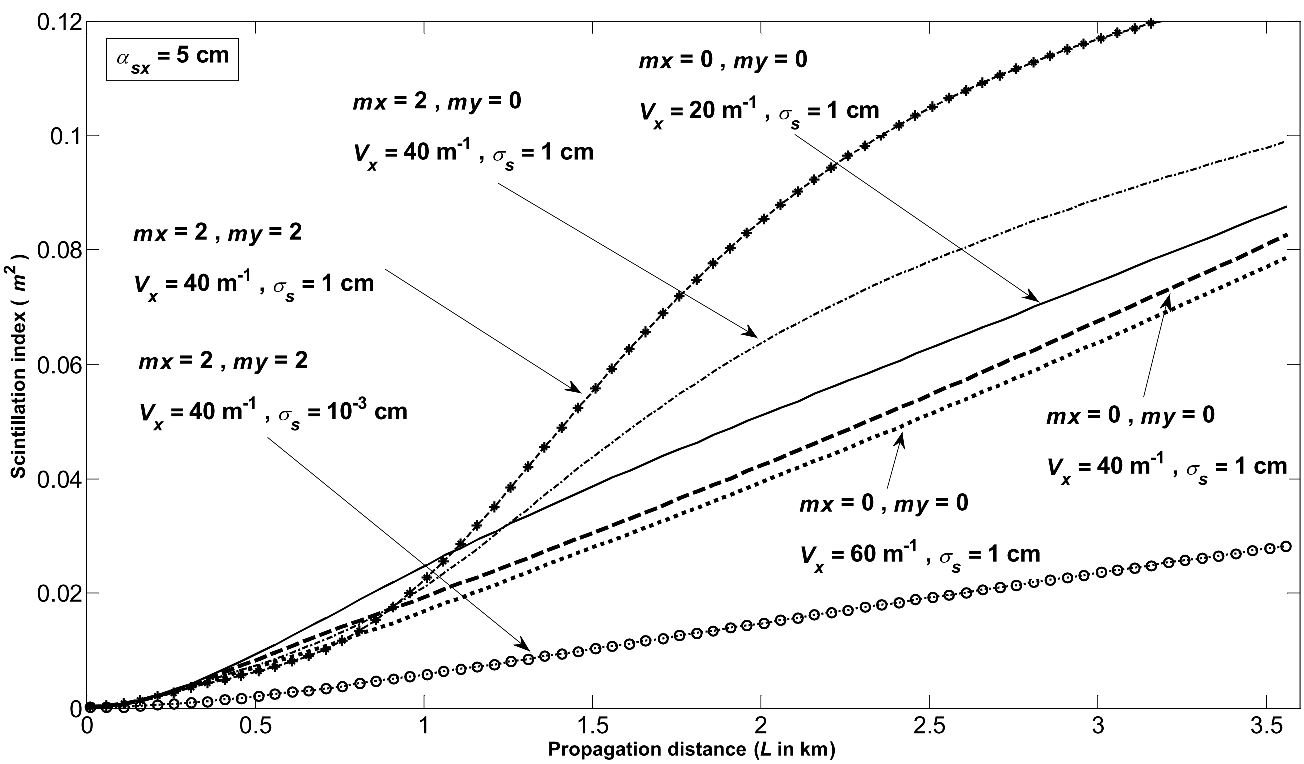

Fig. 5 Scintillation index behavior of partially coherent higher-order sine Gaussian beams against propagation distance

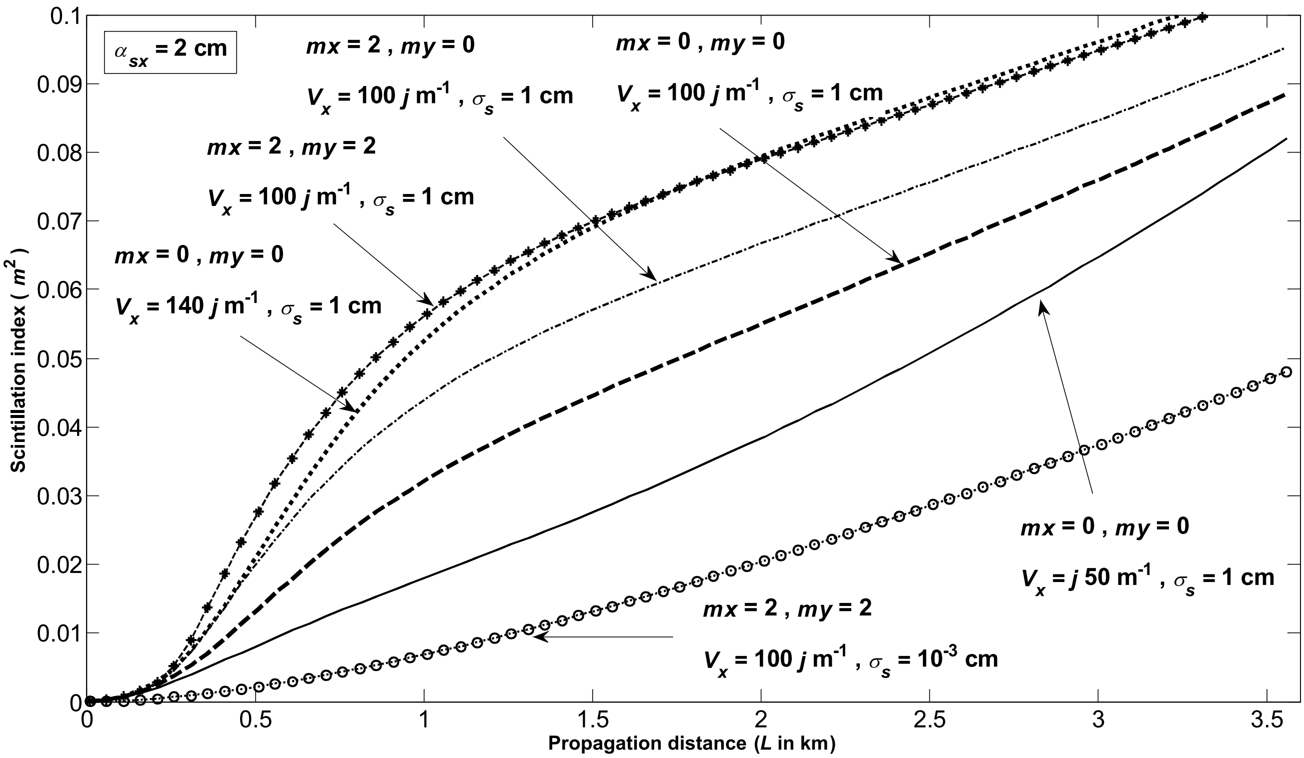

Fig. 6 Scintillation index behavior of partially coherent higher-order sinh Gaussian beams against propagation distance

Finally, we investigate the dependence of scintillations on source sizes for cos, cosh, sine, and sinh beams at specific values of displacement parameter and propagation distance, namely $V_x = 1/\alpha_{sx}$, $L = 2.5$ km. In this context, Fig. 7 shows that for cos Gaussian beams partial coherence is advantageous in terms of scintillations, particularly at large source sizes, and higher orders serve to reduce scintillations even more at low coherence degrees. A similar appearance emerges in Fig. 8 for cosh Gaussian beams, except the partially coherent higher-order beam of $mx = 2$, $my = 0$, $\sigma_s = 1$ cm has a bump above the fully coherent beam of $mx = 0$, $my = 0$, $\sigma_s \to \infty$ from a source size approximately $\alpha_{sx} = 4$ cm onwards. In addition, as the curve of $mx = 0$, $my = 0$, $\sigma_s \to \infty$ indicates, the fully coherent beam exhibits a slight peak at a source size around 3 cm. Examining Figs. 7 and 8 jointly, we deduce that for the same set of source and propagation conditions, cos Gaussian beams will scintillate less than the cosh Gaussian ones. The variation of scintillation against the source size of sine Gaussian beams is considered in Fig. 9, where it is seen that higher orders with a partial coherence value of $\sigma_s = 1$ cm will have higher scintillations than fundamental sine Gaussian beams. This reverses however as the coherence degree is lowered. More or less the same behavior is encountered in Fig. 10 that provides the scintillation variation of sinh Gaussian beams against the source size. The comparison of Figs. 9 and 10 reveals that sine Gaussian beams will offer less scintillations than the sinh Gaussian ones. It should be noted that for each individual curve of Figs. 6–10, the partial coherence parameter σ_s is kept constant while the source size is increased as we go from the left side to the right. This means that to the right of Figs. 6–10, the sources effectively become less coherent, a property that should be born in mind when assessing the falling trend of some of the curves in Figs. 6–10.

4 Conclusion

The scintillation properties in weak atmospheric turbulence of partially coherent general beams are examined using the extended Huygens–Fresnel integral and self-designed Matlab function. The approach followed enables us to find the scintillation indices of partially coherent higher-order beams and their fundamental versions of sinusoidal Gaussian and annular types in semi-analytical form. Our results indicate that the on-axis scintillations of coherent cos Gaussian beams are smaller than the on-axis scintillations of Gaussian beams when the displacement parameter magnitude is increased, however this trend reverses for the higher-order cases at shorter propagation distances. Behavior of coherent cosh Gaussian scintillations is the opposite of cos Gaussian scintillations where the intensity fluctuations of cosh Gaussian beams will be higher at larger displacement

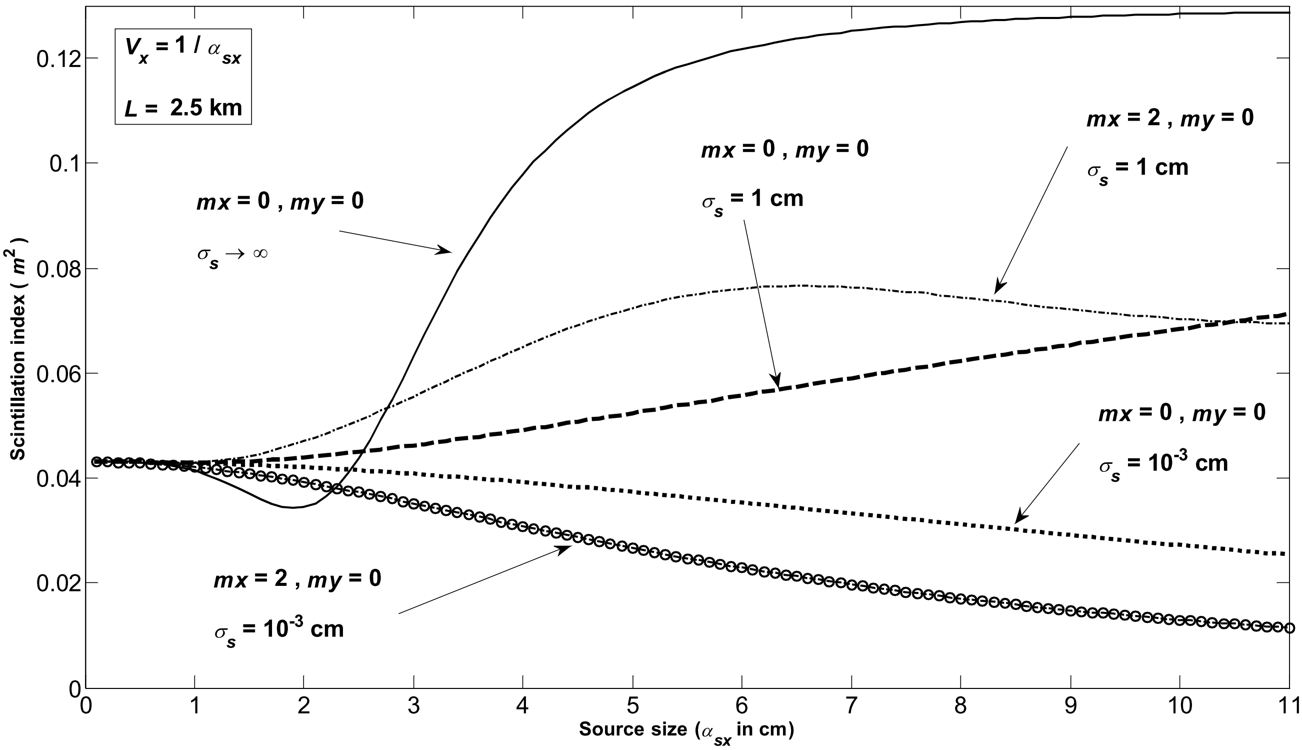

Fig. 7 Scintillation index behavior of fully and partially coherent higher-order cos Gaussian beams against source size

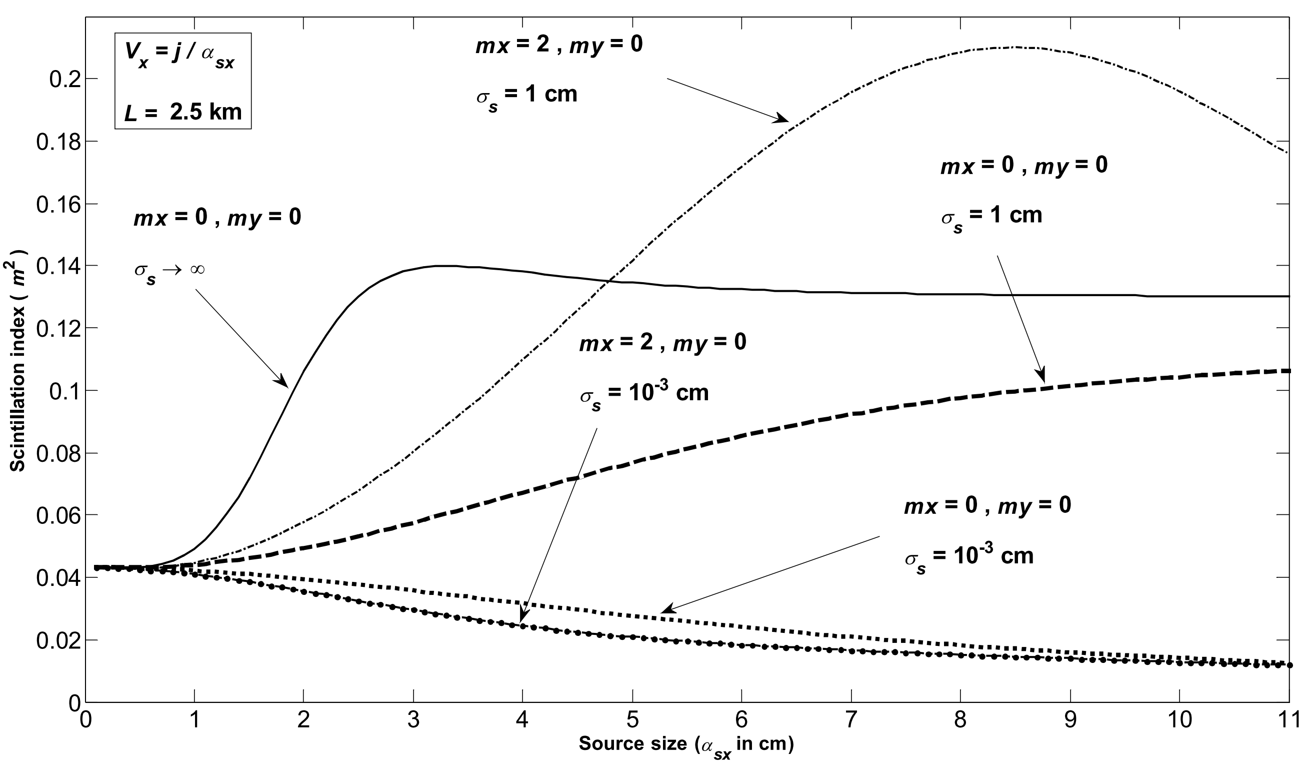

Fig. 8 Scintillation index behavior of fully and partially coherent higher-order cosh Gaussian beams against source size

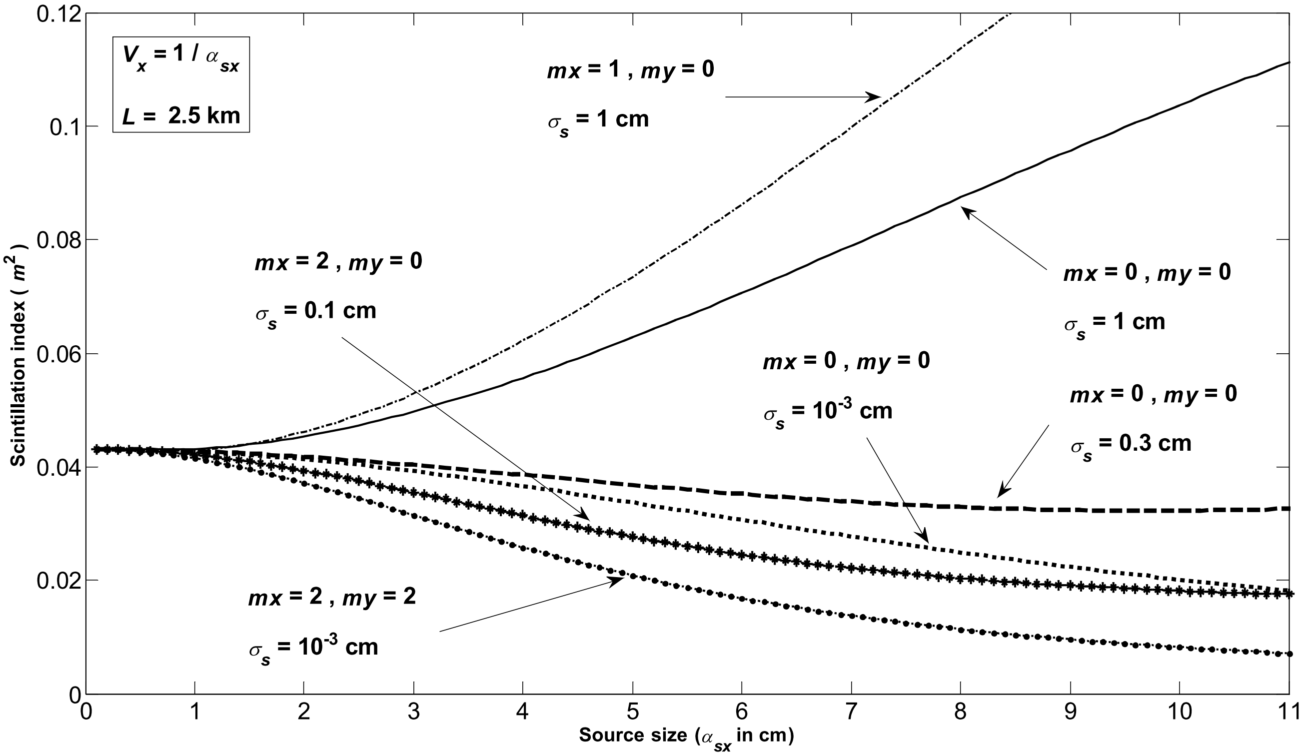

Fig. 9 Scintillation index behavior of partially coherent higher-order sine Gaussian beams against source size

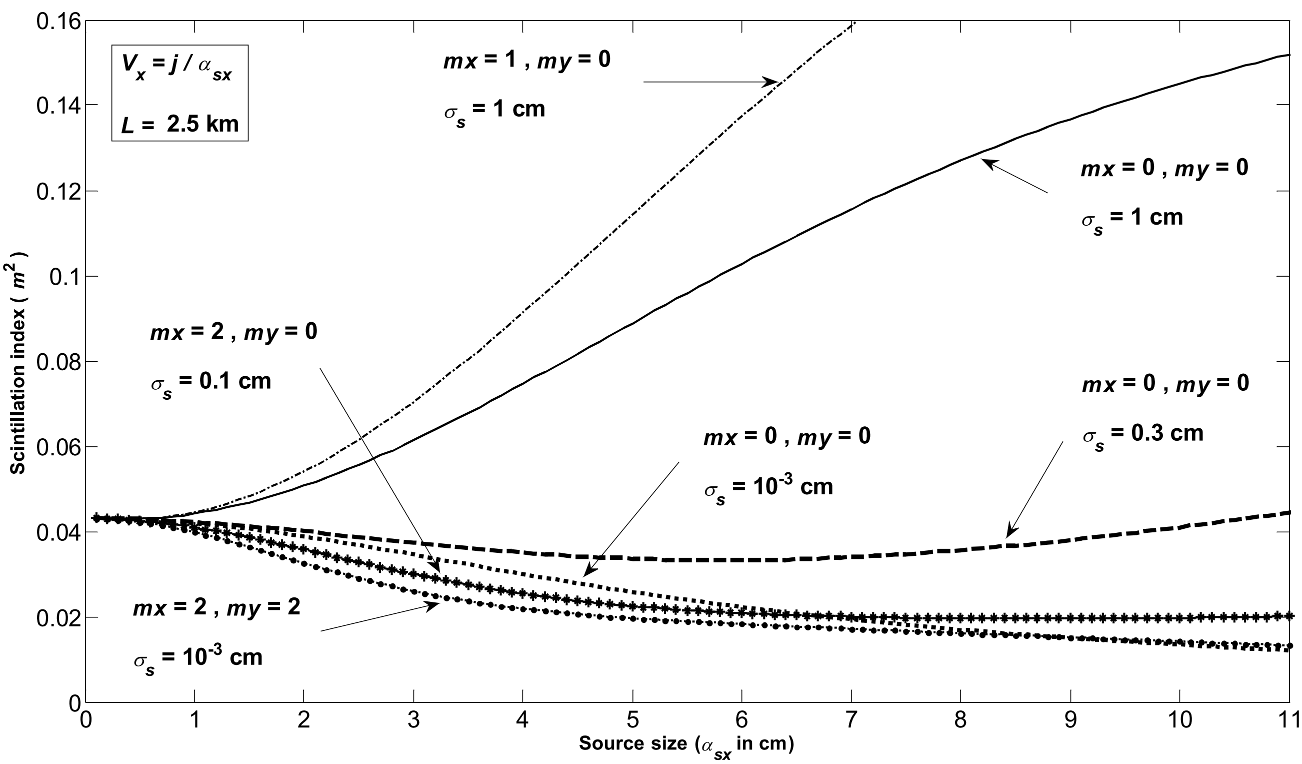

Fig. 10 Scintillation index behavior of partially coherent higher-order sinh Gaussian beams against source size

parameters and the scintillations of the higher-order versions are larger than the scintillations of the fundamental beam counterparts. It is observed that the higher-order coherent annular beams will scintillate less than the fundamental counterparts. For low coherence higher-order annular beams, the scintillations tend to attain close scintillation index values as the orders vary. Partially coherent higher-order sine Gaussian beams exhibit reduction in scintillations as the displacement parameter is increased. However, keeping the partial coherence parameter fixed will cause increase in scintillations for higher orders. Substantial decrease in the intensity fluctuations is observed when the coherence parameter attains a small value. For partially coherent higher-order sinh Gaussian beams, the scintillations increase as the displacement parameter increases, the higher orders also causing more scintillations.

Examining the scintillations versus the source size and taking the displacement parameter equal to the inverse of the source size, one sees that for cos and cosh Gaussian beams, partial coherence brings advantages especially at large source sizes. For higher-order beams scintillations are reduced even more at low coherence degrees, except that the partially coherent higher-order cosh Gaussian beam may exhibit a bump above the coherent counterpart. Examining the scintillation index of partially coherent higher-order sine Gaussian and sinh Gaussian beams versus source size reveals that higher orders at a fixed partial coherence value exhibit higher scintillations than the fundamental beam counterparts, however, this trend seems to be reversed as the coherence degree becomes smaller. It can be said of all the beams, as the source becomes less coherent, the scintillations decrease. Although this fact was revealed earlier for plane, spherical and Gaussian beams [3], thus may seem trivial in this sense, here we stress that its verification for the types of beams of this study have been reported by us for the first time. Also, use of higher-order beams will generally result in smaller scintillations, especially for less coherent sources.

Acknowledgements The work in this paper was performed as a part of The Scientific and technological Research Council of Turkey (TUBİTAK) grant number 108E130. H.T. Eyyuboğlu and Y. Baykal gratefully acknowledge their support and the hosting provided by Çankaya University.

Yangjian Cai acknowledges the support by the National Natural Science Foundation of China under Grant No. 10904102, the Foundation for the Author of National Excellent Doctoral Dissertation of PR China under Grant No. 200928, the Natural Science of Jiangsu Province under Grant No. BK2009114 and the Huo Ying Dong Education Foundation of China under Grant No. 121009.

We are particularly grateful to Dr. Peter Jonathan Starr for copy editing the manuscript.

References

1. C.G. Little, Mon. Not. R. Astron. Soc. **111**, 289 (1951)
2. D.L. Fried, Appl. Opt. **10**, 721 (1971)
3. L.C. Andrews, R.L. Phillips, *Laser Beam Propagation through Random Media* (SPIE, Bellingham, 2005)
4. V.I. Tatarski, *Wave Propagation in a Turbulent Medium* (McGraw–Hill, New York, 1961)
5. D.L. Fried, J. Opt. Soc. Am. A **57**, 175 (1967)
6. A. Ishimaru, *Wave Propagation and Scattering in Random Media, Vol. 2* (Academic Press, New York, 1978)
7. J.W. Goodman, *Stat. Opt.* (Wiley, New York, 1985)
8. G.R. Ochs, R.J. Hill, Appl. Opt. **24**, 2430 (1985)
9. J.H. Churnside, S.F. Clifford, Appl. Opt. **27**, 4884 (1988)
10. J.R. Dunphy, J.R. Kerr, J. Opt. Soc. Am. A **63**, 981 (1973)
11. R.J. Hill, S.F. Clifford, J. Opt. Soc. Am. **71**, 675 (1981)
12. P.J. Titterton, J. Opt. Soc. Am. **63**, 439 (1973)
13. M.S. Belen'kii, J. Opt. Soc. Am. A **11**, 1150 (1994)
14. R.K. Tyson, J. Opt. Soc. Am. A **19**, 753 (2002)
15. J.H. Churnside, R.J. Lataitis, J.J. Wilson, Appl. Opt. **31**, 4285 (1992)
16. T. Wang, G.R. Ochs, R.S. Lawrence, Appl. Opt. **20**, 4073 (1981)
17. A.A. Tokovinin, J. Opt. Soc. Am. A **20**, 686 (2003)
18. G.J. Baker, J. Opt. Soc. Am. A **23**, 395 (2006)
19. K. Kiasaleh, J. Opt. Soc. Am. A **23**, 557 (2006)
20. A.S. Gurvich, M.S. Belen'kii, J. Opt. Soc. Am. A **12**, 2517 (1995)
21. A. Consortini, G. Conforti, J. Opt. Soc. Am. A **1**, 1075 (1984)
22. V.S.R. Gudimetla, J.F. Holmes, M.E. Fossey, P.A. Pincus, Appl. Opt. **31**, 1286 (1992)
23. R.G. Frehlich, S.M. Wandzura, R.J. Hill, J. Opt. Soc. Am. A **4**, 2158 (1987)
24. F.S. Vetelino, L.C. Andrews, Proc. SPIE **5160**, 86 (2004)
25. Y. Baykal, H.T. Eyyuboğlu, Appl. Opt. **45**, 3793 (2006)
26. L.C. Andrews, R.L. Phillips, C.Y. Hopen, *Laser Beam Scintillation with Applications* (SPIE, Bellingham, 2001)
27. D.C. Cowan, L.C. Andrews, Opt. Eng. **47**, 026001 (2008)
28. H.T. Eyyuboğlu, Y. Baykal, Appl. Opt. **46**, 1099 (2007)
29. Y. Cai, Y. Chen, H.T. Eyyuboğlu, Y. Baykal, Opt. Lett. **32**, 2405 (2007)
30. H.T. Eyyuboğlu, Y. Baykal, J. Opt. Soc. Am. A **24**, 156 (2007)
31. S.A. Arpali, H.T. Eyyuboğlu, Y. Baykal, J. Mod. Opt. **55**, 227 (2008)
32. H.T. Eyyuboğlu, Y. Baykal, Y. Cai, Appl. Phys. B **91**, 265 (2008)
33. H.T. Eyyuboğlu, E. Sermutlu, Y. Baykal, Y. Cai, O. Korotkova, Appl. Phys. B **93**, 605 (2008)
34. H.T. Eyyuboğlu, Y. Baykal, E. Sermutlu, O. Korotkova, Y. Cai, J. Opt. Soc. Am. A **26**, 387 (2009)
35. Y. Cai, H.T. Eyyuboğlu, Y. Baykal, J. Opt. Soc. Am. A **25**, 1497 (2008)
36. Y. Chen, Y. Cai, H.T. Eyyuboğlu, Y. Baykal, Appl. Phys. B **90**, 87 (2008)
37. H.T. Eyyuboğlu, Y. Baykal, E. Sermutlu, Y. Cai, Appl. Phys. B **92**, 229 (2008)
38. Y. Baykal, M.A. Plonus, J. Opt. Soc. Am. A **2**, 2124 (1985)
39. V.I. Klyatskin, V.I. Tatarskii, Radiophys. Quantum Electron. **13**, 1061 (1970)
40. V.A. Banakh, G.M. Krekov, V.L. Mironov, S.S. Khmelevtsov, R.Sh. Tsvik, J. Opt. Soc. Am. **64**, 516 (1974)
41. W.B. Miller, J.C. Ricklin, L.C. Andrews, J. Opt. Soc. Am. A **11**, 2719 (1994)
42. V.P. Aksenov, V.A. Banakh, V.L. Mironov, Sov. J. Quantum Electron. **6**, 1233 (1978)
43. V.A. Banakh, V.L. Mironov, Sov. J. Quantum Electron. **8**, 875 (1978)
44. J.C. Leader, J. Opt. Soc. Am. **69**, 73 (1979)
45. J.C. Leader, J. Opt. Soc. Am. **71**, 542 (1981)
46. R.L. Fante, Opt. Acta **28**, 1203 (1981)
47. Y. Baykal, M.A. Plonus, S.J. Wang, Radio Sci. **18**, 551 (1983)
48. S.J. Wang, Y. Baykal, M.A. Plonus, J. Opt. Soc. Am. **73**, 831 (1983)

49. P. Polynkin, A. Peleg, L. Klein, T. Rhoadarmer, J. Moloney, Opt. Lett. **32**, 885 (2007)
50. C.Y. Young, Y.V. Gilchrest, B.R. Macon, Opt. Eng. **41**, 1097 (2002)
51. Y. Baykal, H.T. Eyyuboğlu, Y. Cai, Appl. Opt. **48**, 1943 (2009)
52. Y. Baykal, H.T. Eyyuboğlu, Y. Cai, J. Mod. Opt. (2010). doi:10.1080/09500340903521850
53. Y. Baykal, H.T. Eyyuboğlu, C.Z. Çil, Y. Cai, O. Korotkova, unpublished
54. Y. Baykal, J. Opt. Soc. Am. A **23**, 889 (2006)
55. Ç. Arpali, C. Yazıcıoğlu, H.T. Eyyuboğlu, S.A. Arpali, Y. Baykal, Opt. Express **14**, 8918 (2006)
56. Y. Baykal, H.T. Eyyuboğlu, Opt. Commun. **269**, 30 (2007)
57. H.T. Eyyuboğlu, Y. Baykal, Opt. Commun. **278**, 17 (2007)
58. H.T. Eyyuboğlu, E. Sermutlu, Appl. Phys. B **98**, 865 (2010)